PENSOFT.

MUSEUM FÜR
NATURKUNDE
BERLIN

A comparative description of the mesosomal musculature in Sphecidae and Ampulicidae (Hymenoptera, Apoidea) using 3D techniques

Maraike Willsch[1], Frank Friedrich[2], Daniel Baum[3], Ivo Jurisch[1], Michael Ohl[1]

1 *Museum für Naturkunde Berlin, Invalidenstraße 43, 10115 Berlin, Germany*

2 *Institut für Zoologie, Universität Hamburg, Martin-Luther-King-Platz 3, 20146 Hamburg, Germany*

3 *Zuse Institute Berlin, Takustraße 7, 14195 Berlin, Germany*

http://zoobank.org/94793352-7C43-496C-83D1-A10A355BC801

Corresponding author: Maraike Willsch (maraike.willsch@mfn.berlin)

Abstract

Conflicting hypotheses about the relationships among the major lineages of aculeate Hymenoptera clearly show the necessity of detailed comparative morphological studies. Using micro-computed tomography and 3D reconstructions, the skeletal musculature of the meso- and metathorax and the first and second abdominal segment in Apoidea are described. Females of *Sceliphron destillatorium*, *Sphex* (*Fernaldina*) *lucae* (both Sphecidae), and *Ampulex compressa* (Ampulicidae) were examined. The morphological terminology provided by the Hymenoptera Anatomy Ontology is used. Up to 42 muscles were found. The three species differ in certain numerical and structural aspects. Ampulicidae differs significantly from Sphecidae in the metathorax and the anterior abdomen. The metapleural apodeme and paracoxal ridge are weakly developed in Ampulicidae, which affect some muscular structures. Furthermore, the muscles that insert on the coxae and trochanters are broader and longer in Ampulicidae. A conspicuous characteristic of Sphecidae is the absence of the metaphragma. Overall, we identified four hitherto unrecognized muscles. Our work suggests additional investigations on structures discussed in this paper.

Key Words

Introduction

Hymenoptera form one of the largest insect orders and comprise more than 150,000 extant species (Aguiar et al. 2013). The group of interest examined in this paper constitutes a subclade of Hymenoptera, the Aculeata (stinging wasps, bees, and ants; Sharkey et al. 2012). Derived from the modified ovipositor, the stinger is a synapomorphy of aculeate Hymenoptera and a key innovation for their evolutionary success (Sharkey et al. 2012; Schmidt 2016). The nature of phylogenetic relationships within the monophyletic Aculeata is still contested (e.g., Königsmann 1978; Lomholdt 1982; Rasnitsyn 1988; Alexander 1992; Brothers and Carpenter 1993; Ronquist et al. 1999; Peters et al. 2011, 2017; Sharkey et al. 2012; Johnson et al. 2013; Branstetter et al. 2017). Traditionally, Aculeata

is divided into three lineages: Chrysidoidea, Vespoidea, and Apoidea (O'Neill 2001; Branstetter et al. 2017).

About 10,000 species of digger wasps (also named apoid wasps) as part of the species-rich superfamily Apoidea are currently known (Pulawski 2020). The most obvious synapomorphy of Apoidea is the rounded pronotal lobe (Ohl and Engel 2007). Apoidea is divided into the monophyletic Anthophila (bees) and the paraphyletic apoid wasps. The latter comprises Ampulicidae, Crabronidae, Heterogynaidae, and Sphecidae (e.g., Branstetter et al. 2017). Recent phylogenomic and molecular analyses suggest Ampulicidae is the sister to the rest of the Apoidea (Debevec et al. 2012 [ribosomal 28S and protein-coding nuclear genes]; Sann et al. 2018 [target DNA enrichment and transcriptomic sequence data]). However, contradictory evidence on the phylogenetic rela-

tionships within the apoid wasps (e.g., Lohrmann et al. 2008; Ohl and Spahn 2010; Debevec et al. 2012; Sharkey et al. 2012; Branstetter et al. 2017) remains unresolved. Based upon different research methods, most results suggest, that Sphecidae and Ampulicidae are well-supported clades (Ohl and Spahn 2010 [morphological study]; Branstetter et al. 2017 [ultraconserved element phylogenomics]; Peters et al. 2017 [protein-coding genes]), whereas Crabronidae are likely to be paraphyletic (Lohrmann et al. 2008 [nuclear long-wavelength-opsin and mitochondrial cytochrome-c-oxidase]; Debevec et al. 2012; Branstetter et al. 2017; Peters et al. 2017). However, Sann et al. (2018) found Crabronidae to be polyphyletic. Another unresolved issue is the position of Heterogynaidae within Apoidea (Ohl and Bleidorn 2006). Debevec et al. (2012) obtained two different results: Heterogynaidae nested within Crabronidae (maximum likelihood tree) and as sister to a monophyletic group of Sphecidae *sensu stricto*, Crabronidae and Anthophila (Bayesian tree). The first result was already proposed by Ohl and Bleidorn (2006 [long-wavelength opsin]). Branstetter et al. (2017) found Heterogynaidae to be sister to a grouping of paraphyletic Crabroninae and Sphecidae.

Morphological characters are still one of the major sources of phylogenetic inference (e.g., Friedrich and Beutel 2010; Ohl and Spahn 2010; Vilhelmsen et al. 2010; Zimmermann and Vilhelmsen 2016; Liu et al. 2019). Nevertheless, internal mesosomal structures are insufficiently studied across Hymenoptera, as predicated by Vilhelmsen et al. (2010), who provided detailed information for many apocritan wasps and other Hymenoptera; especially the mesosomal musculature of *Pison chilense* (Crabronidae) and external mesosomal characters for *Pison chilense*, *Stangeella cyaniventris* (Sphecidae), and *Ampulex compressa* (Ampulicidae) are described. They demonstrated, that the mesosomal region reveals considerable information for phylogenetic research. Previously, indispensable work about the mesosomal musculature in Hymenoptera was presented by Maki (1938), Snodgrass (1942; in particular, for *Apis*), Heraty (1989), and Matsuda (1970), followed by Prentice (1998). Recent substantial work was accomplished by Mikó et al. (2007). They dissected the musculature of the head and mesosoma in a review of the parasitic wasp family Scelionidae. Furthermore, a reinterpretation of the delimitation of the metapostnotum in Chrysidoidea was presented by Kawada et al. (2015). Moreover, Porto et al. (2016) defined internal mesosomal characters of bees and evaluated the potential of these structures, concluding that they are of great value to phylogenetic investigations. Garcia et al. (2017) described several body parts of three new species of the rare ant genus *Zasphinctus*, resulting in a comparative character matrix for species-level taxonomy. Subsequently, Liu et al. (2019) provided insights on the mesosoma of an ant worker of *Myrmecia* for comparisons with other Aculeata and to gain new information about evolution and body function.

A state-of-the-art method for morphological analyses is the three-dimensional imaging, using micro-computed tomography (microCT). It is a highly powerful technique

(Faulwetter et al. 2013 and references therein; Garcia et al. 2017; Liu et al. 2019), as it makes internal structures visible without destroying the specimen. Moreover, the digital 3D models can be created repeatedly to work on different goals and the data can easily be shared worldwide.

By using 3D imaging, we aim to expand the basic morphological knowledge for phylogenetic investigations within Aculeata. In this paper we present data of muscular structures in the mesosoma of *Sceliphron destillatorium* (Illiger, 1807), *Sphex* (*Fernaldina*) *lucae* de Saussure, 1867 (both Sphecidae), and *Ampulex compressa* (Fabricius, 1781) (Ampulicidae) (Fig. 1). These wasps are solitary and nest-provisioning predators with different lifestyles (e.g., Williams 1942; Bohart and Menke 1976; Fouad et al. 1994; Haspel and Libersat 2003; Libersat 2003; Ohl and Spahn 2010). Both families were selected for their large number of plesiomorphic characters within digger wasps (Ohl and Spahn 2010), which might help to reconstruct the ancestral apoid anatomy. Primarily, we illustrate and describe mesosomal conformations of the skeletal musculature, with focus on the mesothorax, metathorax, and the first abdominal segment (propodeum). We also describe muscles that originate in the mesosoma and insert in the second abdominal segment (metasoma) because of strong interrelations of these muscles in this transition zone between both tagmata. The wasp waist allows for increased movability of the abdomen and, therefore, is an important anatomical cluster for various physical activities requiring precise movements of the abdomen below the body. This includes, for instance, stinging prey or enemies for defence, laying eggs (Williams 1942; Bohart and Menke 1976), carrying prey between mid or hind legs and abdomen while in flight, dragging prey forwards or backwards (Bohart and Menke 1976), and increasing balance in flight (at least when the second abdominal segment is petiolate; Bohart and Menke 1976).

Material and methods

Specimens and body parts examined

Sphex and *Ampulex* were taken from the collection of the Museum für Naturkunde Berlin (MfN) and *Sceliphron* was collected in the field (Table 1). To examine and compare the muscle sets, specimens of the same sex (females) were selected. We analysed the musculature of the mesothorax, metathorax, and the first and second abdominal segments.

Preparation, microCT, and 3D reconstruction

The extremities of the specimens were removed to minimize the scan field for optimizing the resolution of the data sets. Furthermore, the tip of the gaster was removed to facilitate the infiltration of the iodine, which intensifies the visibility of the musculature in the scan. Following Metscher (2009) and Gignac et al. (2016), our specimens were contrasted in a 25% iodine solution in pure ethanol

Dtsch. Entomol. Z. 67 (1) 2020, 51–67

53

Figure 1. Portraits of the three specimens examined, lateral view. **A.** *Sceliphron destillatorium*, body size 20 mm; **B.** *Sphex* (*Fernaldina*) *lucae*, body size 18 mm; **C.** *Ampulex compressa*, body size 21 mm.

Table 1. Basic information about the specimen collection, classification, preparation, and settings for microCT scanning.

Specimens	*Sceliphron destillatorium*	*Sphex (Fernaldina) lucae*	*Ampulex compressa*
MfN collection number	MfN_Hym_Sph_I004239	MfN_Hym_Sph_I000635	MfN_Hym_Amp_I000029
Location/label data	GREECE, Crete, Afrata [little road], 35°34'38.31"N, 23°4'2.3"E	USA, New Mexico, Hidalgo Co., Gray Ranch, 20.6 mi S Ammas	GERMANY, Berlin, MfN breed, Oviposition 6 Aug. 2015, Eclosion 27 Sept. 2015
Date of collection	24 June 2015	28 Aug. 2003	28 Sept. 2015
Leg.	M. Willsch	S. Schiller, I. Richert	L. Kirschey
Det.	M. Willsch 2015	M. Ohl 2004	L. Kirschey 2015
Family	Sphecidae	Sphecidae	Ampulicidae
Sex	Female	Female	Female
Body size (mm)	20	18	21
Storage	96% ethanol	96% ethanol	96% ethanol
Sample preparation	25% Iodine staining, critical point drying	25% Iodine staining, critical point drying	25% Iodine staining, critical point drying
Scanning medium	Air	Air	Air
Voltage (kV)	48	48	50
Current (µA)	250	250	275
Number of images	1000	1000	1440
Rotation steps	0.36	0.36	0.25
Exposure time (ms)	1000	1000	1000
Resolution (µm/pixel)	3.40	4.69	5.00

(100%) for three days and washed out with pure ethanol for 30 seconds. The wasps were dried using a critical point dryer (Leica EM CPD300; Table 1). Afterwards, the three specimens were scanned at the Visualisation Laboratory of the MfN using a Phoenix nanotom X-ray|s tube (General Electric) at 48–50 kV and 250–275 µA. At 1 second per image 1000–1440 projections were generated per scan. The different kV- and projection-settings depended on the respective specimen size, which was also responsible for the range of the effective voxel size between 3.4–5 µm (Table 1). The cone beam reconstruction was performed using the CT reconstruction software PHOENIX|X-RAY DATOS|X version 2.0 (GE Sensing & Inspection Technologies GmbH).

3D segmentation and post-processing

The raw microCT image data were visualised and analysed by using a Wacom Cintiq 22HD interactive pen display and the software AMIRA ZIB EDITION 2020.02 and former versions (provided by the Zuse Institute Berlin). All muscles were segmented and labelled manual-

ly by using appropriate segmentation tools in AMIRA. Segmented materials were transformed into high-resolution surfaces using the Isosurface-Tool in AMIRA. The reconstruction was accomplished for one body side of the specimens, as no structural asymmetries were observed in this region. Therefore, the number of muscles given in the results refers to one-half of the body. For post-editing (e.g., picture artefacts, file size reduction, file converting, figure compilation) we exported TIF-files from AMIRA into ADOBE PHOTOSHOP CS6.

Terminology

Skeletal musculature was categorised based on insertion sites. The muscle terminology of the Hymenoptera Anatomy Ontology (HAO; http://portal.hymao.org/projects/32/public/ontology/) (Mikó et al. 2007; Vilhelmsen et al. 2010; Yoder et al. 2010; Seltmann et al. 2012) has been adopted here. In this connection, we provide a list of Universal Resource Identifiers (URI) for each muscular and cuticular term (Suppl. material 1: Table S1). It was created by using the "analyze" tool on the HAO website. Newly

detected muscles, not listed in the HAO so far or found in other literature, were also named in the HAO-scheme by the areas of origin and insertion with additional topographical orientation, if required (Table 2). The abbreviations used for the designation of muscles and sclerite structures are composed of the basic terms as follows:

Region of origin and insertion:

3ax2	third axillary sclerite of fore wing
3ax3	third axillary sclerite of hind wing
ba	basalare
cx	coxa
fu	furca
ism	intersegmental membrane
occ	occlusor
pc	pectus
ph	phragma
pl	pleuron
S	sternum
s	thoracal sternum
sa	subalare
sp	spiracle
T1	first abdominal tergite/propodeum
T2	second abdominal tergite
tr	trochanter

Divided thorax:

1	located on the prothorax
2	located on the mesothorax
3	located on the metathorax

Positions:

a	anterior
d	dorsal
l	lateral
m	medial
p	posterior
v	ventral

Order; mostly stated for functional groups of muscles:

a or **1**	first
b or **2**	second
c or **3**	third

Descriptions, that involve the meso- and metafurca, are based on the terminology of Porto et al. (2016). The descriptions in the results were ordered by the point of insertion from mesosoma towards metasoma and by relevant functional groups, if possible (Table 2). In this comparative work, *Sceliphron destillatorium* serves as reference species (Fig. 2). In addition, a homologisation with the generalised nomenclature for the thoracic musculature of Neoptera following Friedrich and Beutel (2008) is presented in Table 2.

Data availability

The large image data sets accomplished for this study are available online as a data publication in conjunction with this paper. Thus, our images and raw data are freely accessible via the MfN data repository (Willsch 2019; https://doi.org/10.7479/dft0-yy6m). Moreover, images will be available on the HAO portal (http://portal.hymao.org).

Results

We found 42 muscle pairs within the analysed tagmata of the three species (Table 2). There are 37 muscles in *Sceliphron* (mesothorax 18, metathorax 14, first and second abdominal segments 5), 39 in *Ampulex* (mesothorax 19, metathorax 16, first and second abdominal segments 4), and 40 muscles in *Sphex* (mesothorax 20, metathorax 15, first and second abdominal segments 5). The following description of the skeletal musculature in *Sceliphron* serves as structural basis. Subsequently, comparative descriptions of differing muscles in *Sphex* and *Ampulex* are given. Each muscle absent in one or two of the compared species examined is mentioned below (see also Table 2):
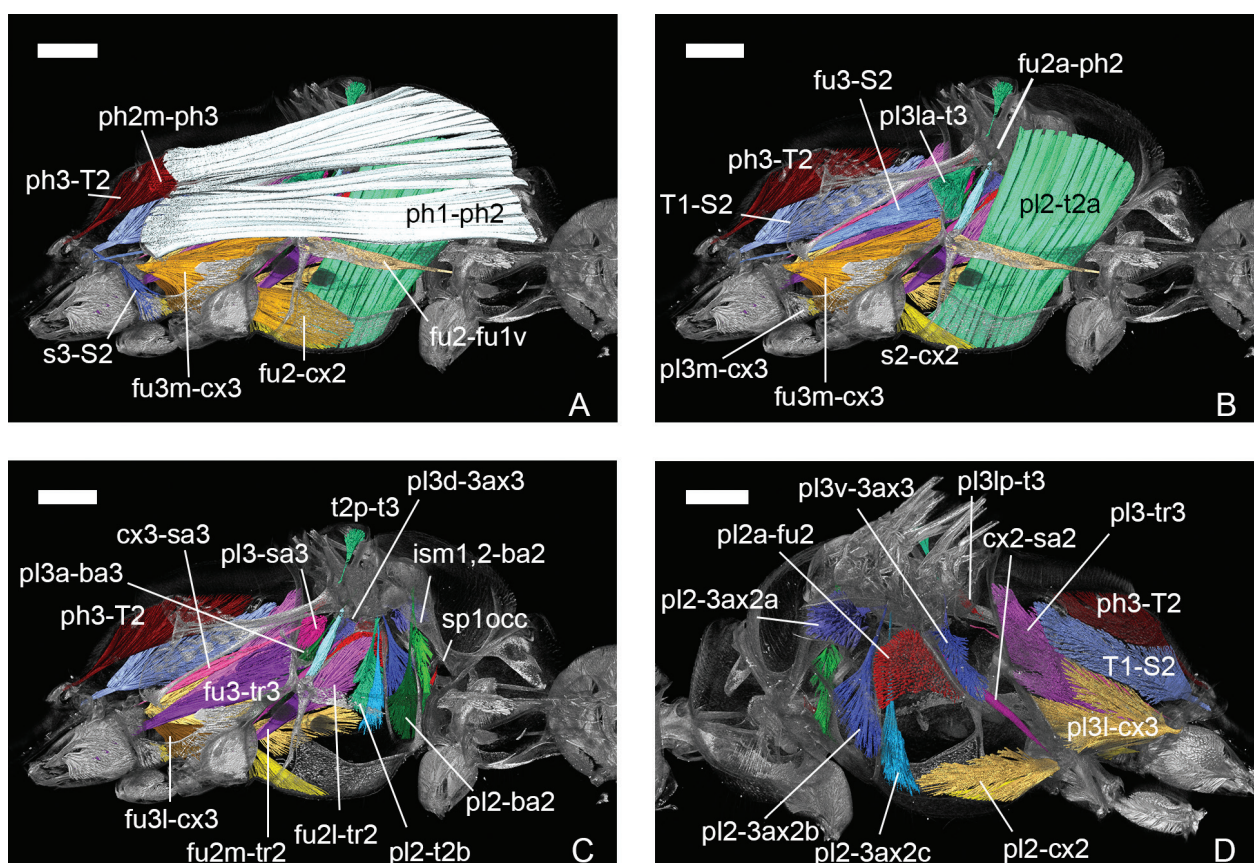
Sceliphron destillatorium (Illiger, 1807)

Mesothorax. Ventral mesofurco-profurcal muscle (fu2-fu1v; Fig. 3A) arises ventromedially from the mesofurcal bridge, then runs horizontal and inserts ventrally on the base of the profurca. **First mesopleuro-mesonotal muscle (pl2-t2a**; Fig. 3B) arises from the mesopectus and inserts on the mesoscutum. The muscle expands vertically and is the second largest muscle in the mesothorax. **Mesopleuro-mesobasalar muscle (pl2-ba2**; Fig. 3C) arises anteroventrally from the mesopleuron, fuses with ism1,2-ba2, and inserts on the mesobasalare anterior to the pleural wing articulation. **Anterior thoracic spiracle occlusor muscle (sp1occ**; Fig. 3C) arises proximally of the intersegmental membrane anteromedial to ism1,2-ba2, runs obliquely, and inserts posteriorly on the anterior thoracic spiracle. Externally, the spiracle is covered by the pronotal lobe. **Intersegmental membrane-mesobasalar muscle (ism1,2-ba2**; Fig. 3C) arises from both the intersegmental membrane between the pronotum and mesopectus, and from the mesopleuron, and inserts on the mesobasalare after fusing with pl2-ba2. **First mesopleuro-third axillary sclerite of fore wing muscle (pl2-3ax2a**; Fig. 3D) arises anterodorsally from the mesopleuron and inserts on the third axillary sclerite of the fore wing; it is short and fan-shaped. **Second mesopleuro-third axillary sclerite of fore wing muscle (pl2-3ax2b**; Fig. 3D) arises anterolaterally from the mesopleuron. This vertical, fan-shaped muscle is situated ventral to pl2-3ax2a and inserts on the third axillary sclerite of the fore wing. **Third mesopleuro-third axillary sclerite of fore wing muscle (pl2-3ax2c**; Fig. 3D) arises
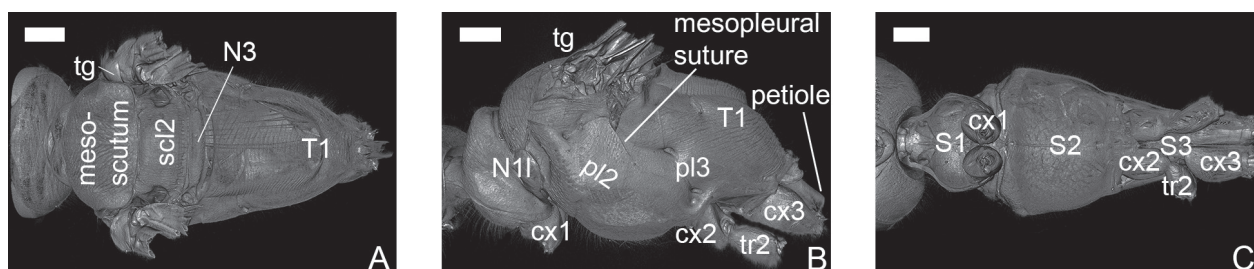
Figure 2. Volume rendering of the mesosomal exoskeleton of *Sceliphron destillatorium*, anterior to the left. **A.** Dorsal surface view; **B.** Lateral surface view; **C.** Ventral surface view. Abbreviations: **N1l** – pronotal lobe, **N3** – metanotum, **cx1** – procoxa, **cx2** – mesocoxa, **cx3** – metacoxa, **pl2** – mesopleuron, **pl3** – metapleuron, **tr2** – mesotrochanter, **S1** – prosternum, **S2** – mesosternum, **S3** – metasternum, **scl2** – mesoscutellum, **T1** – propodeum, **tg** – tegula. Scale bars: 0.9 mm (A, B), 1 mm (C).

Figure 3. *Sceliphron destillatorium*, volume rendering, mesosomal musculature, **A–C:** medial view, anterior to the right, **D:** lateral view, anterior to the left. **A.** Muscles discernible from the centre; **B.** Muscles positioned sublateral; **C.** Muscles located sublateral and lateral; **D.** Laterally positioned muscles. Abbreviations: **fu2-fu1v** – ventral mesofurco-profurcal; **pl2-t2a** – first mesopleuro-mesonotal; **pl2-ba2** – mesopleuro-mesobasalar; **sp1occ** – anterior thoracic spiracle occlusor; **ism1,2-ba2** – intersegmental membrane-mesobasalar; **pl2-3ax2a** – first mesopleuro-third axillary sclerite of fore wing; **pl2-3ax2b** – second mesopleuro-third axillary sclerite of fore wing; **pl2-3ax2c** – third mesopleuro-third axillary sclerite of fore wing; **pl2-t2b** – second mesopleuro-mesonotal; **cx2-sa2** – mesocoxo-mesosubalar; **fu2a-ph2** – anterior mesofurco-mesolaterophragmal; **pl2a-fu2** – anterior mesopleuro-mesofurcal; **pl2-cx2** – mesopleuro-mesocoxal; **s2-cx2** – mesosterno-mesocoxal; **fu2-cx2** – mesofurco-mesocoxal; **fu2l-tr2** – lateral mesofurco-mesotrochanteral; **fu2m-tr2** – median mesofurco-mesotrochanteral; **ph1-ph2** – prophragmo-mesophragmal; **pl3a-ba3** – anterior metapleuro-metabasalar; **t2p-t3** – posterior mesonoto-metanotal; **pl3la-t3** – anterolateral metapleuro-metanotal; **pl3d-3ax3** – dorsal metapleuro-third axillary sclerite of hind wing; **pl3-sa3** – metapleuro-metasubalar; **cx3-sa3** – metacoxo-metasubalar; **pl3m-cx3** – median metapleuro-metacoxal; **fu3l-cx3** – lateral metafurco-metacoxal; **fu3m-cx3** – median metafurco-metacoxal; **pl3l-cx3** – lateral metapleuro-metacoxal; **fu3-tr3** – metafurco-metatrochanteral; **pl3-tr3** – metapleuro-metatrochanteral; **ph2m-ph3** – median mesophragmo-metaphragmal; **ph3-T2** – metaphragmo-second abdominal tergal; **T1-S2** – propodeo-second abdominal sternal; **fu3-S2** – metafurco-second abdominal sternal; **s3-S2** – metasterno-second abdominal sternal. Scale bars: 0.8 mm (A–C), 0.9 mm (D).

Table 2. Terminology of the thoracic and abdominal musculature of all specimens examined. Origination and insertion are described on the basis of *Sceliphron*. If a muscle is absent in *Sceliphron*, the description refers to *Sphex* or *Ampulex*, respectively, if absent in *Sphex*. The list is sorted caudad (from thorax towards abdomen) by insertions of the muscles and by assumed functional groups. X = muscle present; - = muscle absent; ? = uncertain homology. A homologisation with the generalised nomenclature for neopteran thoracic muscles of Friedrich and Beutel (2008) is presented.

Abbreviation	Name of muscle	Origin	Insertion	*Sceliphron destillatorium*	*Sphex lucae*	*Ampulex compressa*	Neoptera terminology
Mesothorax							
fu2-fu1v	ventral mesofurco-profurcal	mesofurcal bridge	profurca	X	X	X	Ivlm7
pl2-t2a	first mesopleuro-mesonotal	mesopectus	mesoscutum	X	X	X	IIdvm1
pl2-ba2	mesopleuro-mesobasalar	mesopleuron	mesobasalare	X	X	X	IIspm1
sp1occ	anterior thoracic spiracle occlusor	intersegmental membrane	anterior thoracic spiracle	X	X	X	–
ism1,2-ba2	intersegmental membrane-mesobasalar	intersegmental membrane, mesopleuron	mesobasalare	X	X	X	IIppm2
pl2-3ax2a	first mesopleuro-third axillary sclerite of fore wing	mesopleuron	third axillary sclerite of fore wing	X	X	X	IItpm7
pl2-3ax2b	second mesopleuro-third axillary sclerite of fore wing	mesopleuron	third axillary sclerite of fore wing	X	X	X	IItpm9
pl2-3ax2c	third mesopleuro-third axillary sclerite of fore wing	mesopleuron	third axillary sclerite of fore wing	X	X	X	IItpm9
pl2-t2b	second mesopleuro-mesonotal	mesopleuron	lateral axillar area of mesonotum	X	X	X	IItpm5
cx2-sa2	mesocoxo-mesosubalar	mesocoxa	mesosubalare	X	X	X	IIdvm6
fu2a-ph2	anterior mesofurco-mesolaterophragmal	mesofurcal arm	mesolaterophragma	X	X	X	IIdvm8
sp3occ	posterior thoracic spiracle occlusor	mesofurcal arm	posterior thoracic spiracle	–	X	X	–
pl2a-fu2	anterior mesopleuro-mesofurcal	mesopleuron, mesepimeral ridge	mesofurcal arm	X	X	X	IIspm2
pl2-cx2	mesopleuro-mesocoxal	mesopleuron	mesocoxa (anterolateral)	X	X	X	IIpcm4
pl2-cx2b*	second mesopleuro-mesocoxal	mesopleuron, mesopleural spiracle apodeme	mesocoxa (dorsolateral)	–	X	X[d]	IIpcm4?
s2-cx2	mesosterno-mesocoxal	mesodiscrimenal lamella, mesopectus	mesocoxa (anterolateral)	X	X	X	IIscm3
fu2-cx2	mesofurco-mesocoxal	mesodiscrimenal lamella	mesocoxa (anteromedial)	X	X	X	IIscm2
fu2l-tr2	lateral mesofurco-mesotrochanteral	mesopleuron, mesofurcal arm	mesotrochanteral apodeme (lateral)	X	X[d]	–	IIscm6
fu2m-tr2	median mesofurco-mesotrochanteral	mesofurcal arm	mesotrochanteral apodeme (lateral)	X	X	X[d]	IIscm6
ph1-ph2	prophragmo-mesophragmal	prophragma	mesophragma	X	X	X	IIdlm1
Number of mesothoracic muscles (max. 20):				18	20	19	
Metathorax							
pl3a-ba3	anterior metapleuro-metabasalar	metapleuron, paracoxal ridge	metabasalare	X	X	X[d]	IIIspm1
t2p-t3	posterior mesonoto-metanotal	mesoscutellum	mesophragmal spine in metanotum	X	X	X[d]	IIIdlm3
pl3la-t3	anterolateral metapleuro-metanotal	metapleural apodeme, metafurcal arm	metanotal apodeme	X	X	X[d]	IIItpm5
pl3lp-t3	posterolateral metapleuro-metanotal	metapleuron	metanotum	X	X	X[d]	IIItpm6
pl3v-3ax3	ventral metapleuro-third axillary sclerite of hind wing	metapleuron, mesepimeral ridge	third axillary sclerite of hind wing	X	X	X[d]	IIItpm9
pl3d-3ax3	dorsal metapleuro-third axillary sclerite of hind wing	mesepimeral ridge	third axillary sclerite of hind wing	X	X	X	IIItpm7
pl3-sa3	metapleuro-metasubalar	metapleuron, metapleural apodeme	metasubalare	X	X	X[d]	IIItpm11
cx3-sa3	metacoxo-metasubalar	metacoxa (sublateral)	metasubalare	X	X	X	IIIdvm6
pc3l-fu3*	lateral metapecto-metafurcal	metapectus	paracoxal ridge	–	–	X	–
fu3-cx3*	metafurco-metacoxal	metafurcal arm	metacoxa (medial)	–	–	X	IIIscm3?

Abbreviation	Name of muscle	Origin	Insertion	*Sceliphron destillatorium*	*Sphex lucae*	*Ampulex compressa*	Neoptera terminology
pl3m-cx3	median metapleuro-metacoxal	metapectus, metadiscrimenal lamella	metacoxa (ventrolateral)	X	X	X	IIIscm1
fu3l-cx3	lateral metafurco-metacoxal	paracoxal ridge, metadiscrimenal lamella	metacoxa (lateral)	X	X	X^d	IIIscm2
fu3m-cx3	median metafurco-metacoxal	metafurca, metadiscrimenal lamella	metacoxa (medial)	X	X	X^d	IIIscm2
s3-cx3*	metasterno-metacoxal	metadiscrimenal lamella	metacoxa (medial)	–	X	–	IIIscm1?
pl3l-cx3	lateral metapleuro-metacoxal	metapleuron, paracoxal ridge	metacoxa (dorsolateral)	X	X	X	IIIpcm4
fu3-tr3	metafurco-metatrochanteral	metafurcal arm	metatrochanteral apodeme (central)	X	X	X	IIIscm6
pl3-tr3	metapleuro-metatrochanteral	metapleuron, metapleural apodeme	metatrochanteral apodeme (central)	X?	X?	X^d?	IIIpcm6
Number of metathoracic muscles (max. 17):				14	15	16	
First and second abdominal segment							
ph2m-ph3	median mesophragmo-metaphragmal	mesophragma	median process	X	X	–	IIIdlm1
ph3-T2	metaphragmo-second abdominal tergal	propodeum	second abdominal tergite	X	X	X	–
T1-S2	propodeo-second abdominal sternal	propodeum	second abdominal sternite (lateral)	X	X	X	–
fu3-S2	metafurco-second abdominal sternal	metafurcal arm	second abdominal sternite (ventro-submedial)	X	X	X^d	IIIvlm2
s3-S2	metasterno-second abdominal sternal	metadiscrimenal lamella, metasternum	second abdominal sternite (lateral)	X	X	X^d	–
Number of first and second abdominal segment muscles (max. 5):				5	5	4	
Total number of muscles (max. 42):				37	40	39	

* = newly identified; d = difference in structure or position, amplified in chapter Results

laterally from the mesopleuron, positioned farther ventral and posterior to pl2-3ax2b, and inserts on the third axillary sclerite of the fore wing. It is the most extended and fan-shaped of the three fore wing muscles. **Second mesopleuro-mesonotal muscle (pl2-t2b**; Fig. 3C) arises, somewhat dorsal to pl2-3ax2c, from the mesopleuron, is fan-shaped and inserts on the ventral surface of the lateral axillar area of the mesonotum. **Mesocoxo-mesosubalar muscle (cx2-sa2**; Fig. 3D) arises from the mesocoxal apophysis, which corresponds with the cuticular pit and the paracoxal ridge. This muscle is slim and elongated and inserts on the mesosubalare. **Anterior mesofurco-mesolaterophragmal muscle (fu2a-ph2**; Fig. 3B) arises from the anterodorsal surface of the mesofurcal arm and inserts on the mesolaterophragma. **Posterior thoracic spiracle occlusor muscle (sp3occ)** and the corresponding spiracle (sp2) are absent. The mesopleural pit, which corresponds to the mesopleural apodeme, is visible. **Anterior mesopleuro-mesofurcal muscle (pl2a-fu2**; Fig. 3D) arises from the mesopleuron and from the mesepimeral ridge and inserts on the mesofurcal arm. **Mesopleuro-mesocoxal muscle (pl2-cx2**; Fig. 3D) arises from the mesopleuron and inserts anterolaterally on the mesocoxa. **Second mesopleuro-mesocoxal muscle (pl2-**

cx2b) is absent. **Mesosterno-mesocoxal muscle (s2-cx2**; Fig. 3B) arises mainly from the mesodiscrimenal lamella and partly from the mesopectus; it is located ventrally of pl2-cx2 and inserts anterolaterally on the mesocoxa. **Mesofurco-mesocoxal muscle (fu2-cx2**; Fig. 3A) arises from the mesodiscrimenal lamella as far as the transition to the free basal portion of the mesofurcal arm; it inserts anteromedial on the mesocoxal margin. **Lateral mesofurco-mesotrochanteral muscle (fu2l-tr2**; Fig. 3C) arises partly from the mesopleuron (posteriorly of pl2a-fu2) and partly from the anterior surface of the lateral mesofurcal arm (anteriorly of pl2a-fu2), fuses with the medially adjacent muscle fu2m-tr2, and inserts laterally on the mesotrochanteral apodeme. **Median mesofurco-mesotrochanteral muscle (fu2m-tr2**; Fig. 3C) arises from the posterior surface of the mesofurcal arm and is positioned medially to fu2l-tr2. After fusing with fu2l-tr2, both muscles insert laterally on the mesotrochanteral apodeme. **Prophragmo-mesophragmal muscle (ph1-ph2**; Fig. 3A) arises from the prophragma and inserts on the mesophragma. This horizontal, beam-shaped muscle is the largest in all species examined.

Metathorax. Anterior metapleuro-metabasalar muscle (pl3a-ba3; Fig. 3C) arises from both the meta-

pleuron and from the anterior surface of the paracoxal ridge and inserts on the metabasalare. This longitudinal, lateral muscle extends between the mesopleural and paracoxal ridge. **Posterior mesonoto-metanotal muscle (t2p-t3**; Fig. 3C) arises from the mesoscutellum and inserts laterally on a spine-shaped apodeme, which is located dorsally on the mesophragma at the transition of the meso- and metascutellum; it is fan-like. **Anterolateral metapleuro-metanotal muscle (pl3la-t3**; Fig. 3B) arises anterolaterally from the metapleural apodeme and metafurcal arm and inserts laterally on the metanotal apodeme. It is short and fan-like. Adjacent muscles are fu3-S2 and fu3-tr3, which arise posterior to the metafurcal arm. **Posterolateral metapleuro-metanotal muscle (pl3lp-t3**; Fig. 3D) arises from the metapleuron and inserts on the metanotum by fusing with pl3la-t3, which lies ventral to the small pl3lp-t3. **Ventral metapleuro-third axillary sclerite of hind wing muscle (pl3v-3ax3**; Fig. 3D) arises from the posterior surface of the mesepimeral ridge and the metapleuron. The muscle is located lateral to pl3d-3ax3 and fuses with it, then both insert on the third axillary sclerite of the hind wing. **Dorsal metapleuro-third axillary sclerite of hind wing muscle (pl3d-3ax3**; Fig. 3C) arises dorso-submedial of pl3v-3ax3 from the posterior surface of the mesepimeral ridge, fuses with pl3v-3ax3 along half its length, and inserts on the third axillary sclerite of the hind wing; it is small and compact. **Metapleuro-metasubalar muscle (pl3-sa3**; Fig. 3C) arises from the metapleuron and partly from the metapleural apodeme and inserts on the metasubalare, ventral to the hind wing. **Metacoxo-metasubalar muscle (cx3-sa3**; Fig. 3C) arises from the sublateral margin of the metacoxa and inserts on the metasubalare by fusing with pl3-sa3; it is long and slim. **Lateral metapecto-metafurcal muscle (pc3l-fu3)** and **metafurco-metacoxal muscle (fu3-cx3)** are absent. **Median metapleuro-metacoxal muscle (pl3m-cx3**; Fig. 3B) arises ventromedially from the metapectus and from the metadiscrimenal lamella, inserts ventrolaterally on the metacoxa. **Lateral metafurco-metacoxal muscle (fu3l-cx3**; Fig. 3C) arises sublaterally from the posterior surface of the paracoxal ridge and the metadiscrimenal lamella and inserts laterally on the metacoxa. **Median metafurco-metacoxal muscle (fu3m-cx3**; Fig. 3A, B) arises posteromedially from both the metafurca and metadiscrimenal lamella and inserts medially on the metacoxa. **Metasterno-metacoxal muscle (s3-cx3)** is absent (see *Sphex*). **Lateral metapleuro-metacoxal muscle (pl3l-cx3**; Fig. 3D) arises laterally from the metapleuron and posteriorly from the paracoxal ridge and inserts on the dorsolateral margin of the metacoxa. The muscle is located anteriorly along the metapleural ridge. **Metafurco-metatrochanteral muscle (fu3-tr3**; Fig. 3C) arises posteriorly of the metafurcal arm, inserts centrally on the metatrochanteral apodeme by fusing with pl3-tr3. **Metapleuro-metatrochanteral muscle (pl3-tr3**; Fig. 3D) arises from the metapleuron and partly from the metapleural apodeme, then fuses with fu3-tr3, and inserts centrally on the metatrochanteral apo-

deme. It runs parallel to, and between, pl3l-cx3 and cx3-sa3 and dorsolateral of fu3-tr3.

First and second abdominal segment. Median mesophragmo-metaphragmal muscle (ph2m-ph3; Fig. 3A) arises posteromedially from the mesophragma and inserts anterior to the median process of the propodeum; it is short and square. **Metaphragmo-second abdominal tergal muscle (ph3-T2**; Fig. 3A–D) arises dorsolaterally from the propodeum, inserts dorsally on the second abdominal tergite; it is a large muscle. **Propodeo-second abdominal sternal muscle (T1-S2**; Fig. 3B, D) arises dorsolaterally from the propodeum, right above pl3l-cx3 and laterally of ph3-T2; it is large and inserts on the lateral margin of the second abdominal sternite. **Metafurco-second abdominal sternal muscle (fu3-S2**; Fig. 3B) arises posteriorly from the submedial metafurcal arm, located dorsally of fu3-tr3, and inserts ventro-submedially on the second abdominal sternite; it is elongate and slightly fan-shaped. **Metasterno-second abdominal sternal muscle (s3-S2**; Fig. 3A) arises from the metadiscrimenal lamella and metasternum, inserts on the lateral margin of the second abdominal sternite, and is fan-shaped and bent.

### *Sphex* (*Fernaldina*) *lucae* de Saussure, 1867

Mesothorax. Posterior thoracic spiracle occlusor muscle (sp3occ; Fig. 4A–D) arises medial on the mesepimeral ridge, anterior to the mesofurcal arm, inserts on the posterior thoracic spiracle (sp2), which additionally is surrounded by pl2-t2b (anterodorsal), pl2a-fu2 (posterodorsal), and pl2-cx2b (ventral). The small tracheal occlusor muscle sp3occ is located submedial of pl2a-fu2. **Second mesopleuro-mesocoxal muscle (pl2-cx2b**; first description; Fig. 4A, C, D) arises from the mesopleuron and partly from the mesopleural spiracle apodeme, fuses with pl2-cx2 and inserts dorsolaterally on the mesocoxa; it lies anteroventral to the mesepimeral ridge. **Lateral mesofurco-mesotrochanteral muscle (fu2l-tr2**; Fig. 4A, D) arises from the anterior surface of the mesofurcal arm, runs lateral to fu2m-tr2 and fuses with the same, then both insert laterally on the mesotrochanteral apodeme; fu2l-tr2 is half the size of that in *Sceliphron*.

Metathorax. Lateral metapecto-metafurcal muscle (pc3l-fu3) and **metafurco-metacoxal muscle (fu3-cx3)** are absent. **Metasterno-metacoxal muscle (s3-cx3**; first description; Fig. 4B) arises from the metadiscrimenal lamella and inserts medially on the metacoxa.

Ampulex compressa (Fabricius, 1781)

Mesothorax. Second mesopleuro-mesocoxal muscle (pl2-cx2b; Fig. 5C, D, E, G, H) is slimmer than in *Sphex*. It arises from the mesopleural spiracle apodeme, fuses with pl2-cx2 (Fig. 5A, C, D, G, H), and inserts dorsolaterally on the mesocoxa. **Lateral mesofurco-mesotrochanteral muscle (fu2l-tr2)** is absent. **Median mesofur-
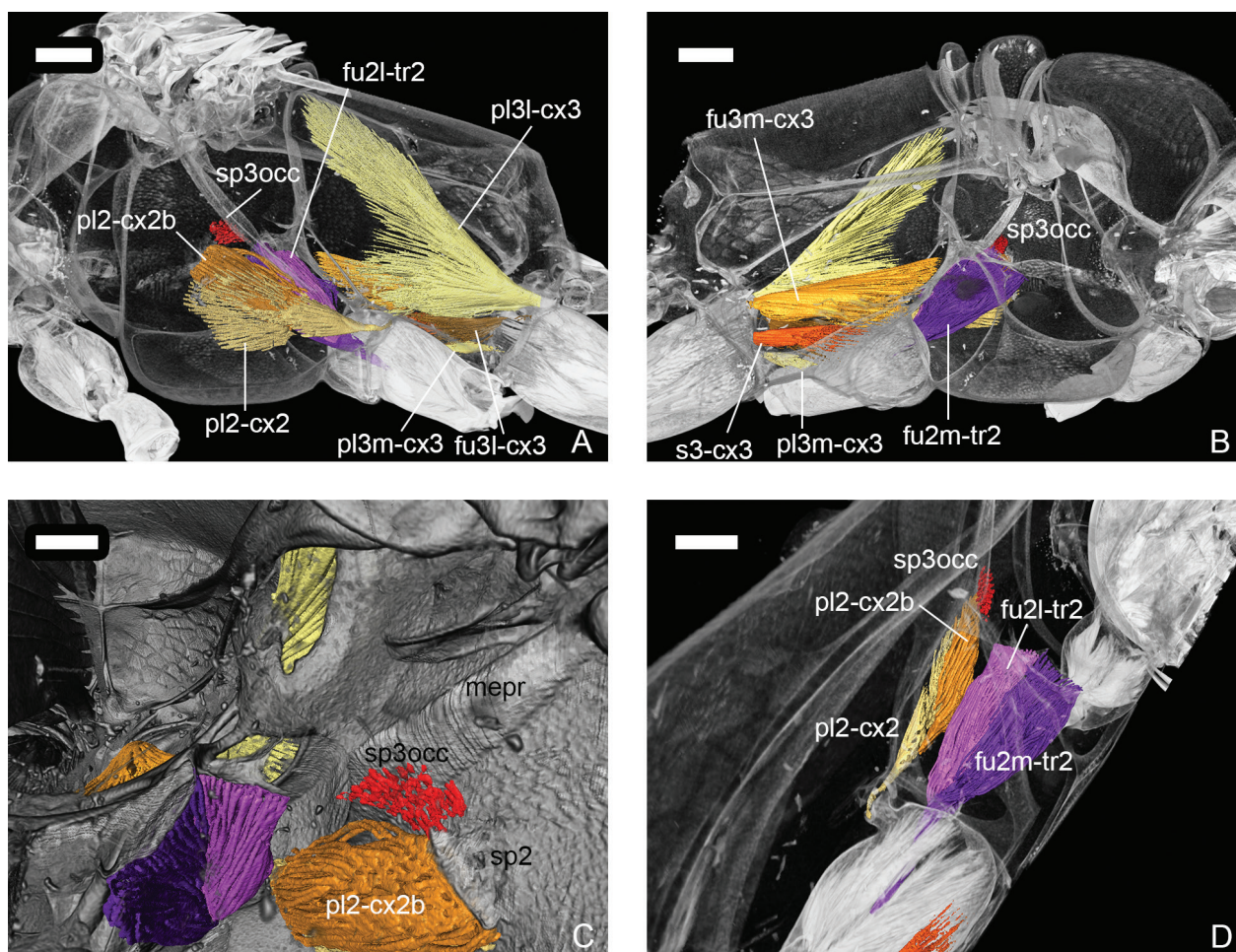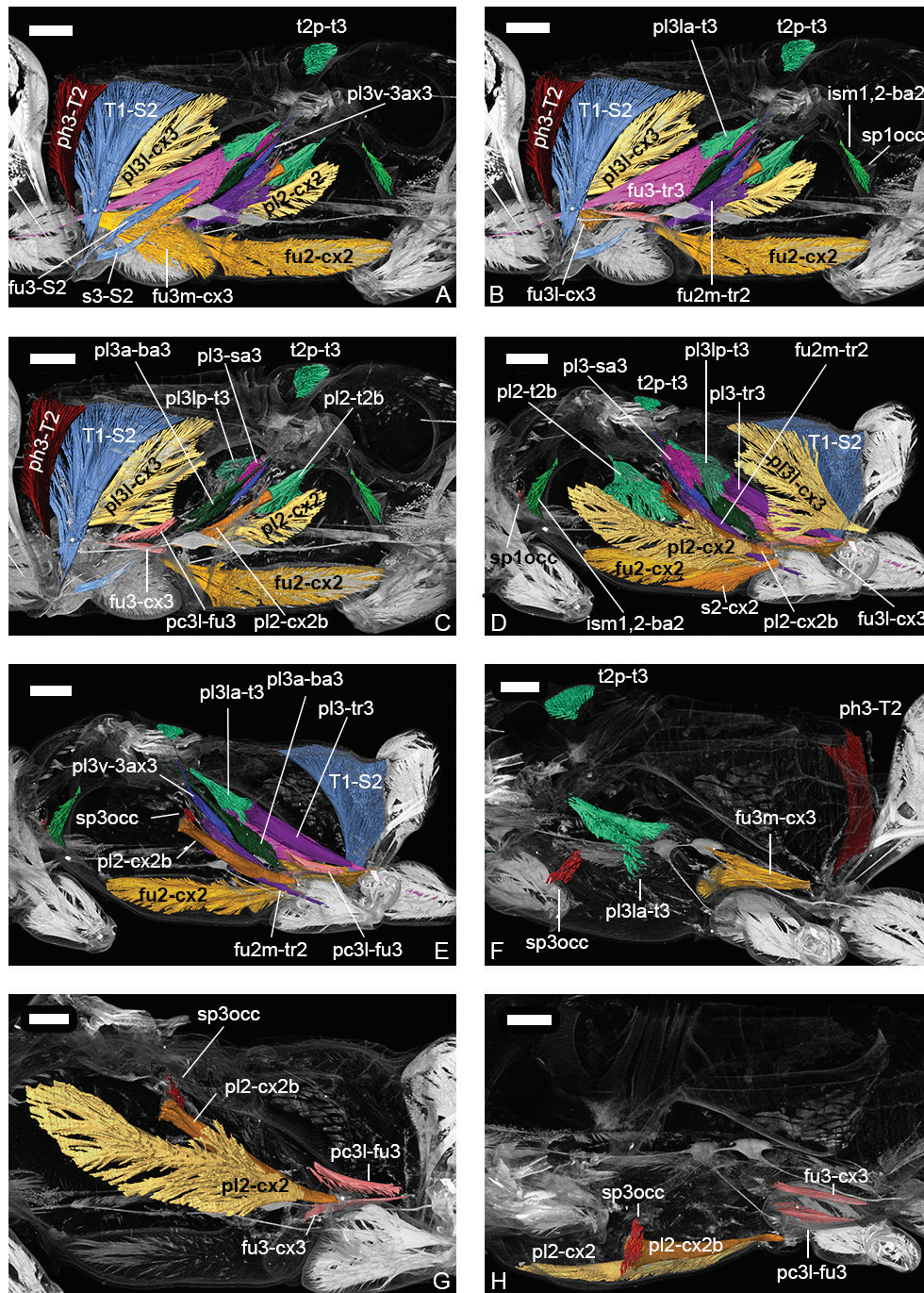
Figure 4. The mesosomal musculature of *Sphex (Fernaldina) lucae* divergent to *S. destillatorium*; volume rendering, transparent exoskeleton. **A.** Lateral view, anterior to the left; **B.** Medial view, anterior to the right; **C.** Anterior view on the posterior thoracic spiracle occlusor; **D.** Dorsomedial view, anterior top right. Abbreviations: **sp3occ** – posterior thoracic spiracle occlusor; **sp2** – posterior spiracle; **pl2-cx2** – mesopleuro-mesocoxal; **pl2-cx2b** – second mesopleuro-mesocoxal; **fu2l-tr2** – lateral mesofurco-mesotrochanteral; **fu2m-tr2** – median mesofurco-mesotrochanteral; **s3-cx3** – metasterno-metacoxal; **pl3m-cx3** – median metapleuro metacoxal; **fu3l-cx3** – lateral metafurco metacoxal; **fu3m-cx3** – median metafurco metacoxal; **pl3l-cx3** – lateral metapleuro metacoxal; **mepr** – mesepimeral ridge. Scale bars: 0.7 mm (A), 0.6 mm (B), 0.3 mm (C), 0.5 mm (D).

co-mesotrochanteral muscle (**fu2m-tr2**; Fig. 5B, D, E) is larger than in Sphecidae, arises from the ventral surface of the mesofurcal arm, and inserts medially on the mesotrochanteral apodeme.

Metathorax. Anterior metapleuro-metabasalar muscle (**pl3a-ba3**; Fig. 5C, E) arises from the metapleuron, posterior to the mesepimeral ridge, and inserts on the metabasalare. This muscle is shorter than in *Sceliphron*, as it originates farther up. The paracoxal ridge is not very distinct. **Posterior mesonoto-metanotal muscle** (**t2p-t3**; Fig. 5A–D, F) arises from the upper sclerite of the mesoscutellum and inserts on the lower surface of the mesoscutellum; rectangular. There is no filament connecting it to another structure. **Anterolateral metapleuro-metanotal muscle** (**pl3la-t3**; Fig. 5B, E, F) mainly arises anterolaterally from the metafurcal arm (touching pl3-tr3 and partly fu3-tr3, which originate on the posterior surface of the metafurcal arm) and partly from the

metapleuron and inserts on the metanotum. **Posterolateral metapleuro-metanotal muscle** (**pl3lp-t3**; Fig. 5C, D) arises from the metapleuron fuses with pl3la-t3, which is covered dorsally by pl3lp-t3, and inserts on the metanotum. It is larger than in *Sceliphron* and *Sphex* and fanshaped. **Ventral metapleuro-third axillary sclerite of hind wing muscle** (**pl3v-3ax3**; Fig. 5A, E) arises from the posterior surface of the mesepimeral ridge. This slim muscle is fused with pl3d-3ax3 and inserts on the third axillary sclerite of the hind wing. **Metapleuro-metasubalar muscle** (**pl3-sa3**; Fig. 5C, D) arises from the metapleuron at the posterior face of the mesepimeral ridge, and inserts on the metasubalare. **Lateral metapecto-metafurcal muscle** (**pc3l-fu3**; first description; Fig. 5C, E, G, H) the slender muscle arises anterior to the metacoxa laterally from the metapectus, and inserts on the posterior surface of the paracoxal ridge. **Metafurco-metacoxal muscle** (**fu3-cx3**; first description; Fig. 5C, G, H) arises medially

Figure 5. The mesosomal musculature of *Ampulex compressa* divergent to Sphecidae; volume rendering, transparent exoskeleton. **A–C** anterior to the right; **D–H** anterior to the left. **A.** Medial view, all relevant muscles visible from the centre; **B.** Medial view on submedial muscles; **C.** Medial view, further lateral located muscles; **D.** All relevant muscles discernible from lateral view; **E.** Muscles located sublateral, lateral view; **F.** Muscles located further medial, lateral view; **G.** All newly identified muscles (plus pl2-cx2), lateral view; **H.** Dorsolateral view on all newly identified muscles (plus pl2-cx2). Abbreviations: **sp1occ** – anterior thoracic spiracle occlusor; **ism1,2-ba2** – intersegmental membrane-mesobasalar; **pl2-t2b** – second mesopleuro-mesonotal; **sp3occ** – posterior thoracic spiracle occlusor; **s2-cx2** – mesosterno-mesocoxal; **pl2-cx2** – mesopleuro-mesocoxal; **pl2-cx2b** – second mesopleuro-mesocoxal; **fu2-cx2** – mesofurco-mesocoxal; **fu2m-tr2** – median mesofurco-mesotrochanteral; **pl3a-ba3** – anterior metapleuro-metabasalar; **t2p-t3** – posterior mesonoto-metanotal; **pl3la-t3** – anterolateral metapleuro-metanotal; **pl3lp-t3** – posterolateral metapleuro-metanotal; **pl3v-3ax3** – ventral metapleuro-third axillary sclerite of hind wing; **pl3-sa3** – metapleuro-metasubalar; **pc3l-fu3** – lateral metapecto-metafurcal; **fu3-cx3** – metafurco-metacoxal; **fu3l-cx3** – lateral metafurco-metacoxal; **fu3m-cx3** – median metafurco-metacoxal; **pl3l-cx3** – lateral metapleuro-metacoxal; **fu3-tr3** – metafurco-metatrochanteral; **pl3-tr3** – metapleuro-metatrochanteral; **ph3-T2** – metaphragmo-second abdominal tergal; **T1-S2** – propodeo-second abdominal sternal; **fu3-S2** – metafurco-second abdominal sternal; **s3-S2** – metasterno-second abdominal sternal. Scale bars: 0.7 mm (A–C), 0.8 mm (D, E), 0.6 mm (F–H).
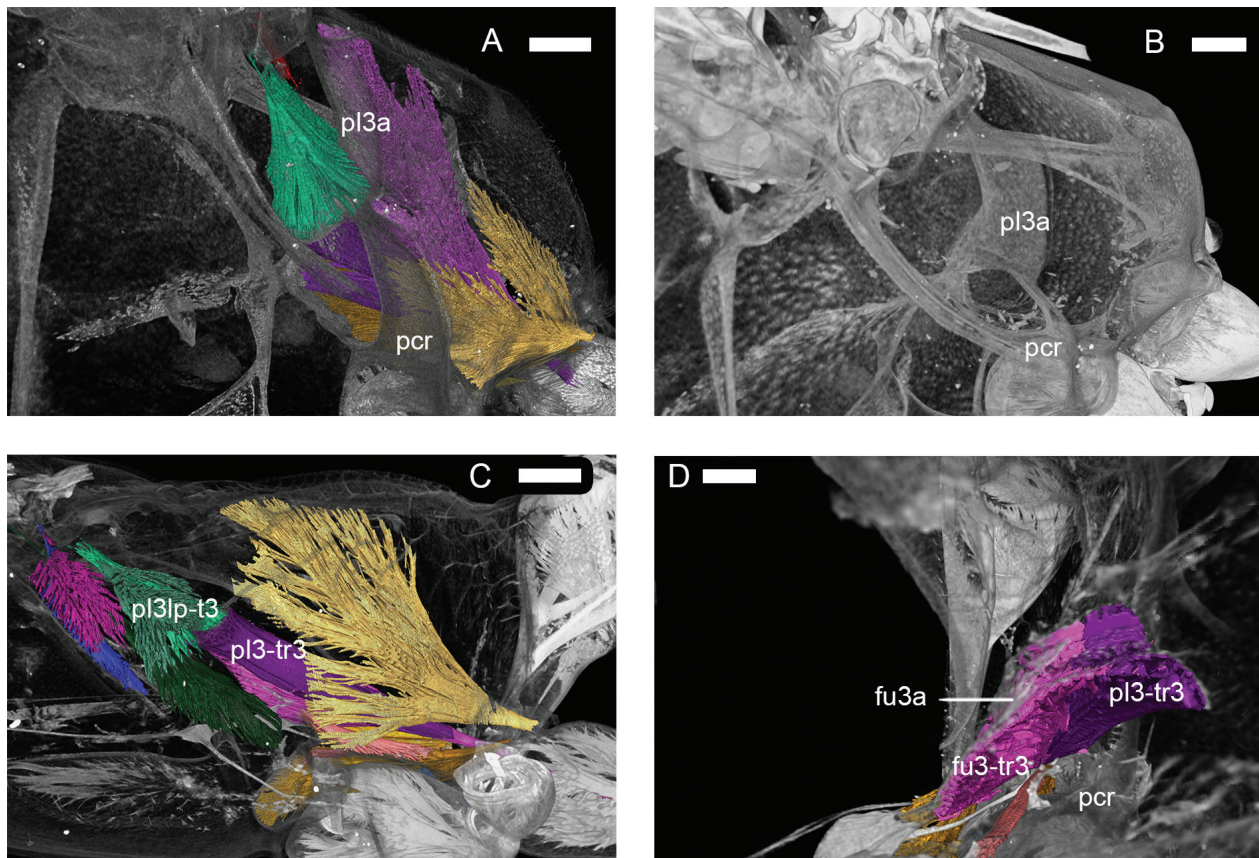
Figure 6. Comparison of the paracoxal ridge (**pcr**) and metapleural apodeme (**pl3a**). **A.** *Sceliphron destillatorium*, anterolateral view, head left; **B.** *Sphex lucae*, anterolateral view, head left; **C.** Weakly developed structures in *Ampulex compressa*, lateral view, head left; **D.** *Ampulex compressa*, paracoxal ridge, lateral metafurcal arms (**fu3a**) fused with reduced metapleural apodeme, anterior view. Further abbreviations: **pl3lp-t3** – posterolateral metapleuro-metanotal muscle, **pl3-tr3** – metapleuro-metatrochanteral muscle, **fu3-tr3** – metafurcor-metatrochanteral muscle. Scale bars: 0.4 mm (A–C), 0.3 mm (D).

from the metafurcal arm, fuses with fu3l-cx3, and inserts medially on the metacoxa; it is slender and flattened. The **median metafurco-metacoxal muscle** (**fu3m-cx3**; Fig. 5A, F) arises posteromedially from the metafurca and from the metadiscrimenal lamella and inserts medially on the metacoxa. The lower metafurcal area runs further cranial and offers more posterior space filled by this muscle. **Lateral metafurco-metacoxal muscle** (**fu3l-cx3**; Fig. 5B, D) arises from the metapectus and inserts dorsolateral on the metacoxa. **Metasterno-metacoxal muscle** (**s3-cx3**) is absent. **Metapleuro-metatrochanteral muscle** (**pl3-tr3**; Fig. 5D, E) arises posteriorly from the metafurcal arm, which merges into a spiracle at that position. The muscle is positioned laterally of fu3-tr3, fuses with it and inserts on the metatrochanteral apodeme. **Metapleural apodeme** and **paracoxal ridge** weakly developed (Fig. 6C, D); **metapleural apodeme** fused with lateral metafurcal arms (Fig. 6D).

Second abdominal segment. Median mesophragmo-metaphragmal muscle (**ph2m-ph3**) is absent. The mesophragma in *Ampulex* is rectangular like the outer cuticle and lacks a posterior notch for the insertion of a muscle. **Metaphragmo-second abdominal tergal muscle** (**ph3-T2**; Fig. 5A–C, F) arises from the metaphragma and propodeum, inserts dorsally on the second abdominal tergite; broad, large muscle extended to the posterior region. **Metafurco-second abdominal sternal muscle** (**fu3-S2**; Fig. 5A) arises posteriorly from the metafurcal arm, positioned posteromedial to fu3-tr3, inserts anteroventrally on the second abdominal sternite. In length and width distinctly more gracile than in *Sceliphron*. **Metasterno-second abdominal sternal muscle** (**s3-S2**; Fig. 5A) arises from the metadiscrimenal lamella and inserts on the anterolateral margin of the second abdominal sternite. It is noticeably smaller and neither fan-like nor bent, as in *Sceliphron*.

Discussion

The cladistic analyses by Vilhelmsen et al. (2010) inferred Crabronidae (*Pison*) as being the closest relative of Sphecidae (*Stangeella*) and Ampulicidae (*Ampulex*) and all three taxa constitute a monophyletic Apoidea. However, many anatomic structures of Ampulicidae and Sphecidae we studied differ significantly from each other, whereas

the two species within Sphecidae show many similarities. Especially, the metathoracic musculature varies remarkably between the families. The muscles that insert on the notum, coxae, and trochanters show distinct structural divergences. Furthermore, the number and origin of muscles varies, due to the less distinct metapleural apodeme and paracoxal ridge in *Ampulex* (additional muscles inserting on the coxae in *Ampulex*: **pl2-cx2b**, **fu3-cx3**; in *Sphex*: **pl2-cx2b**, **s3-cx3**; absent muscle in *Ampulex*: **fu2l-tr2**; origin different in *Ampulex*: **t2p-t3**, **pl3la-t3**, **fu3l-cx3**, **pl3-tr2**; Fig. 3–6; Table 2). In addition, some of the meso- and metacoxal muscles, as well as a mesotrochanteral and a metanotal muscle of *Ampulex* tend to be larger compared to Sphecidae (**pl2-cx2**, **fu2-cx2**, **fu2m-tr2**, **pl3lp-t3**, **fu3m-cx3**, **pl3l-cx3**). The **pl3l-cx3** is also larger in *Sphex* (Fig. 4A) compared to *Sceliphron* (Fig. 3D). Strong levators and depressors attaching on the coxae might be needed for backwards dragging of large prey and speaks for an adaptation to this conspicuous hunting behaviour (Williams 1942). On the contrary, **pl2-cx2b** in *Ampulex* (Fig. 5C, D, E, G, H) is narrower than in *Sphex* (Fig. 4A, C, D); **fu2l-tr2** in *Sphex* is smaller than in *Sceliphron* (Figs 3C, 4A, D). However, muscles supposedly involved in the movement of the notum, coxae, and trochanters should be checked carefully in subsequent studies.

Mesothorax. The mesopleural pit in *Sceliphron* presumably developed by muscle and spiracle reduction. According to Vilhelmsen et al. (2010), the occurrence of the mesopleural pit shows high variances within and amongst superfamilies. Spiracle reduction likely occurred independently in different groups. Snodgrass (1942), for instance, found the posterior thoracic spiracle in honeybee workers without a closing apparatus. Each of the other spiracles is equipped with an occlusor muscle (Snodgrass 1942). Vilhelmsen et al. (2010) documented the absence of the posterior thoracic spiracle in Stephanidae and Pteromalidae, while they evidenced its presence (without **sp3occ**) in the apoid family Crabronidae, as well as in Rhopalosomatidae (Vespoidea), and the non-aculeate families Cynipidae, Evaniidae, and Trigonalidae. Hence, not only Apoidea but also Spheciformes *sensu lato* bear a high variance of the development of this spiracle-muscle-complex. Duncan (1939) presented an illustration of the closing mechanism of the posterior thoracic spiracle in *Vespula*. The occlusor muscles we found in *Sphex* and *Ampulex* (Figs 4A–D, 5F–H) show wider attachment points than the fan-shaped muscle described in Duncan's work. In the neopteran representatives, like *Zorotypus*, examined by Friedrich and Beutel (2008; Table 2), **sp3occ** was not revealed. Concluding, other related specimens should be examined to exclude all doubts about the homologisation of the posterior thoracic spiracle and **sp3occ** and to gain further insights into the different formations.

In all species examined, **pl2-cx2** is located as described by the HAO, with origin on the mesopleuron and anterolateral insertion on the mesocoxa (Figs 3D, 4A, D, 5A, C, D, G, H). However, it is larger and extending farther anteriorly in *Ampulex* (Fig. 5A, C, D, G, H). *Ampulex* distinct-

ly shows the additional and slender mesocoxal muscle **pl2-cx2b**, which we describe here for the first time (Fig. 5C–E, G, H). In *Sphex* it is broader and closely adjacent to **pl2-cx2** (Fig. 4A, C, D). It is absent in *Sceliphron*. Consequently, the development of **pl2-cx2b** should be examined in other species to clarify the phylogenetic relevance.

The muscles **fu2l-tr2** and **fu2m-tr2** in *Ampulex*, which insert on the mesotrochanter, seem to have been coalesced completely, making a separation impossible (compare Fig. 7A, B). Because of the insertion and the rather medial position, we reasonably homologized the structure with **fu2m-tr2** by excluding **fu2l-tr2** for *Ampulex*. The unambiguous identification of both muscles in Sphecidae appears to indicate an autapomorphic feature of Ampulicidae. However, Vilhelmsen et al. (2010; see also references therein) stated that both muscles were found in Evaniidae, Platygastroidea, most Proctotrupoidea, *Plumarius*, and Apoidea, which might include all genera they examined (i.e., *Ampulex*, *Apis*, *Bombus*, *Pison*, *Stangeella*). However, the authors noted the absence of **fu2l-tr2** in *Orthogonalys* (Trigonaloidea) and of **fu2m-tr2** in Ceraphronoidea, Chalcidoidea, and Stephanoidea. Nevertheless, they explained that a secondary subdivision of **fu2m-tr2** may have led to the development of **fu2l-tr2**. In summary, the contrariness referring to **fu2l-tr2** needs to be clarified by additional studies on *Ampulex*, in particular.

In addition, **fu2l-tr2** fills the mesopleural area in *Sceliphron* (Fig. 3C), whereas this muscle is smaller in *Sphex* (Fig. 4A, D). In contrast, **pl2-cx2b** extends over the mesopleural region in *Sphex* and *Ampulex* (Figs 4A, C, D, 5C–E, G, H). In *Ampulex*, the origin of this muscle is the same spiracle apodeme as that from which **sp3occ** arises (Fig. 5E–H); in *Sphex* it partly originates from the posterior thoracic spiracle and partly from the mesopleuron (Fig. 4A, C, D). However, we recommend a closer look at these different formations in other species before drawing phylogenetic conclusions.

Metathorax. The different constructions of the metathoracic muscles mainly depend on variations of the skeletal structures. The slight difference in the metapleural origin of **pl3a-ba3** in *Ampulex* (Fig. 5C, E) is a consequence of the less distinct development of the paracoxal ridge (Fig. 6). As shown by Vilhelmsen et al. (2010), the paracoxal ridge is weakly developed in Ampulicidae and non-apocritan Hymenoptera, whereas it is highly variable within apocritan groups. *Orthogonalys* (Trigonalidae), which serves as reference species in the paper of Vilhelmsen et al. (2010), has a weakly developed paracoxal ridge, except for the ventralmost part. As no other information about the structure in *Pison* (Crabronidae) is available, it should be identical. We confirm the differences noted by Vilhelmsen et al. (2010), as the paracoxal ridge is weakly developed in Ampulicidae and well-marked in Sphecidae (Fig. 6). Additionally, Vilhelmsen et al. (2010) described a distinct paracoxal ridge in Chrysidoidea, Evanioidea, and Stephanoidea.

The muscle **t2p-t3** inserts laterally on a spine, which is located dorsally on the mesophragma in Sphecidae (Fig.
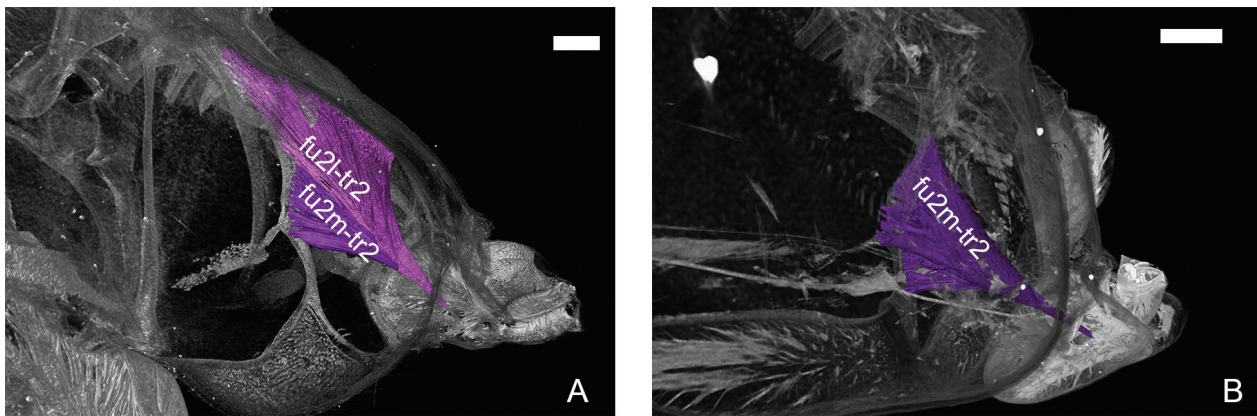
Figure 7. Comparison of **fu2m-tr2** – median mesofurco-mesotrochanteral muscle and **fu2l-tr2** – lateral mesofurco-mesotrochanteral muscle, anterolateral view. **A.** *Sceliphron destillatorium*; **B.** *Ampulex compressa*. Scale bars: 0.4 mm (A), 0.5 mm (B).
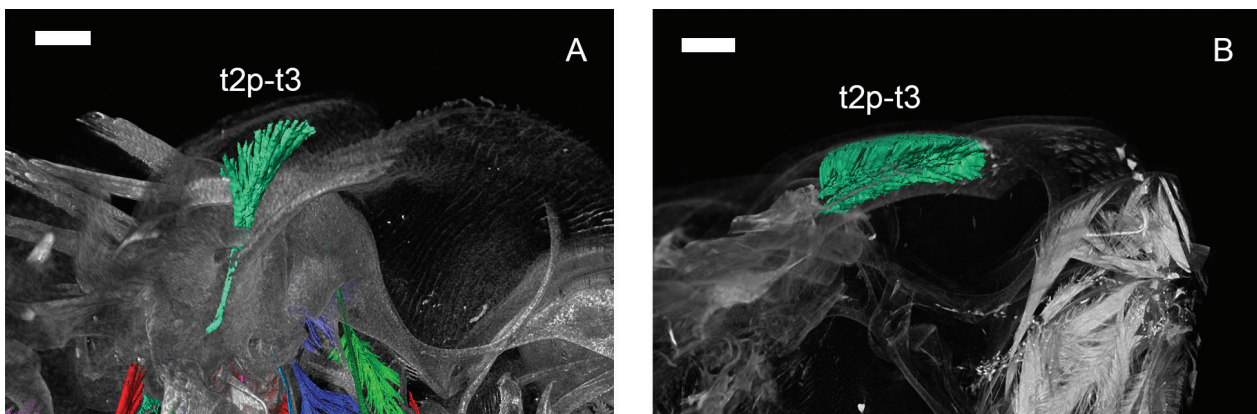

Figure 8. Comparison of **t2p-t3** – posterior mesonoto-metanotal muscle, posteromedial view. **A.** *Sceliphron destillatorium*; **B.** *Ampulex compressa*. Scale bars: 0.2 mm.

8A). Vilhelmsen et al. (2010) revealed in Apoidea and Vespoidea a typical lateral insertion on the metanotum, which is not yet observed in other groups; this might indicate that this feature is synapomorphic in both superfamilies. Although we found the mesoscutellum to be of similar shape in all analysed species, **t2p-t3** in *Ampulex* is instead located entirely between the upper and lower mesoscutellar sclerite (Fig. 8B). So far, this modification seems to be unique. To verify this, further representatives of Ampulicidae should be examined.

The metanotal muscle **pl3la-t3** in *Ampulex* differs from that in Sphecidae because of the weakly developed metapleural apodeme, which leads to a rather more lateral than submedial position on the thorax (Fig. 5B, F). We found a fusion of the lateral metafurcal arms with the metapleural apodeme in *Ampulex* (Fig. 6D), as already observed by Vilhelmsen et al. (2010) in the same species, other apoid taxa (*Stangeella*, *Apis*, *Bombus*, *Pison*), and in Vespoidea. Vilhelmsen et al. (2010) stated that most apocritan Hymenoptera have a metapleural apodeme that is often fused with the lateral metafurcal arms. In non-ap-

ocritan Hymenoptera, the metapleural apodeme shows high morphological diversity. In many cases, this may not be easy to recognize (Vilhelmsen et al. 2010). Studies on more species from both families are necessary to determine if the structures found in the present study are family-specific. Sphecidae has a well-developed metapleural apodeme, similar to Cynipoidea (Vilhelmsen et al. 2010), which is an important characteristic. Our results corroborate the conclusion by Vilhelmsen et al. (2010), that the development of the metapleural apodeme is highly variable within Apocrita and, moreover, even within Apoidea.

Additionally, the weakly developed metapleural apodeme in *Ampulex* influenced the origin of **pl3-sa3**, which only originates from the metapleuron and inserts on the metasubalare (Figs 5C, D, 9B). The origin of the metatrochanteral muscle **pl3-tr3** is also affected in *Ampulex* (Figs 5D, E, 6C, D). This muscle originates from a delicate sclerite, which provides a narrow surface of origin. This sclerite arose from the fusion of the metafurcal arm and metapleural apodeme and is equal to the medial margin of the metapleural apodeme and metafurcal arm.
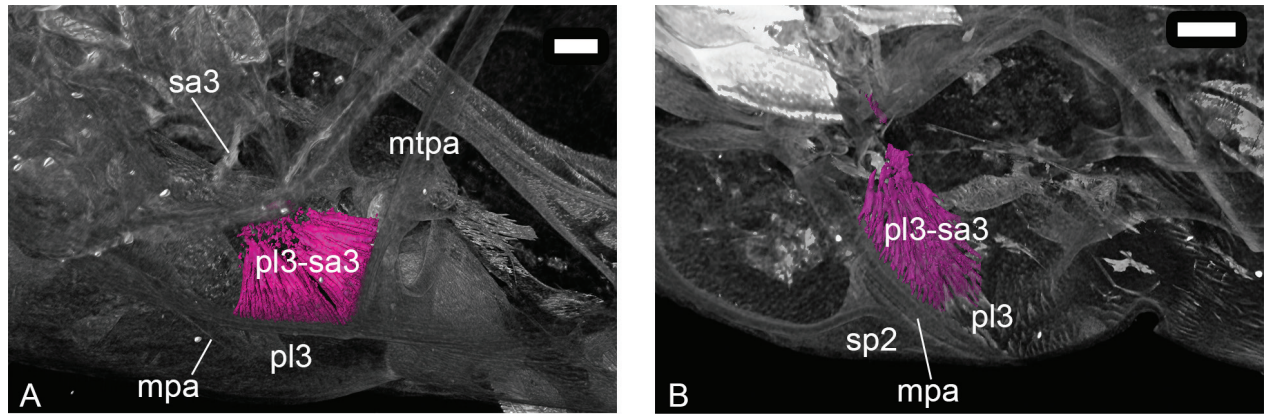
Figure 9. Comparison of **pl3-sa3** – metapleuro-metasubalar muscle, dorsolateral view, anterior to the left. **A.** *Sceliphron destillatorium*; **B.** *Ampulex compressa*. Further abbreviations: **mpa** – mesopleural apodeme; **mtpa** – metapleural apodeme; **pl3** – metapleuron; **sa3** – metasubalare; **sp2** – posterior thoracic spiracle. Scale bars: 0.2 mm (A), 0.4 mm (B).
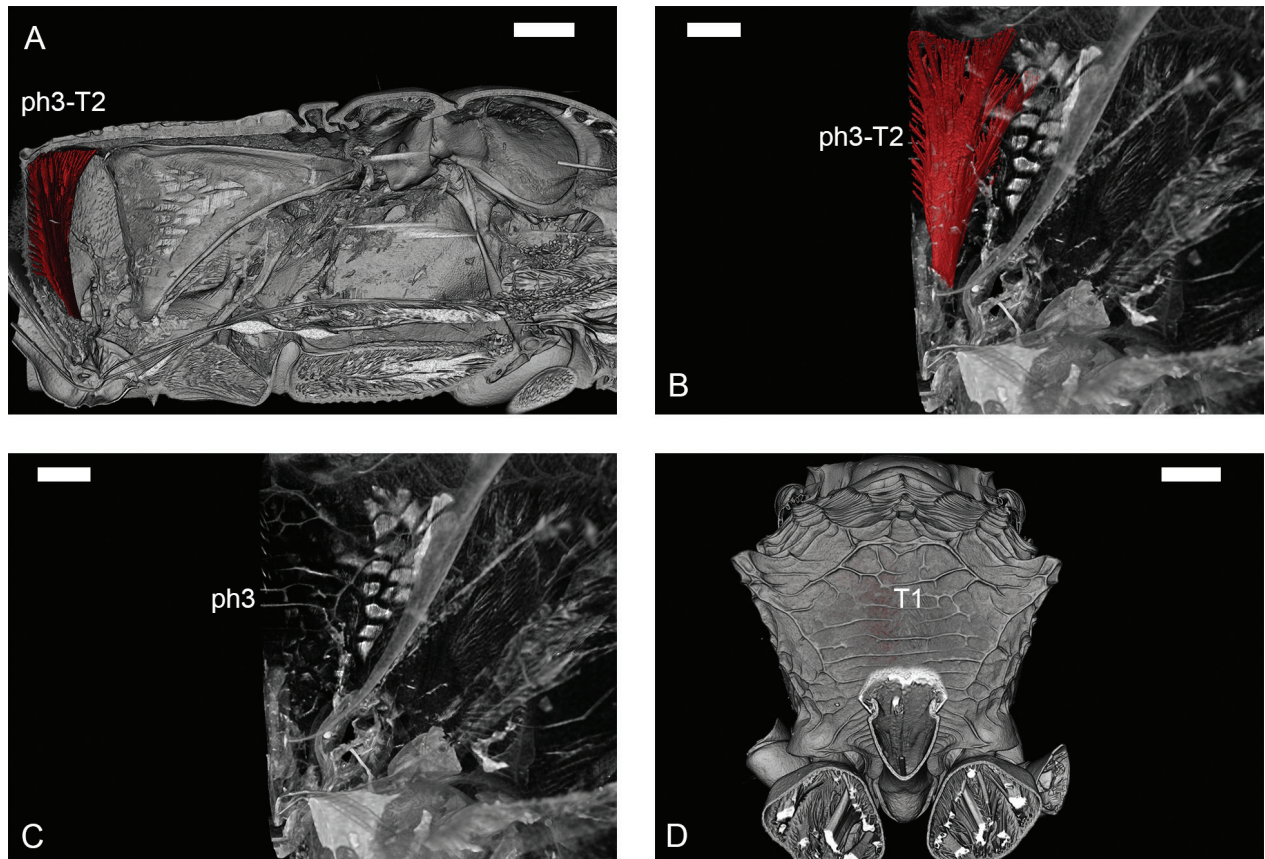
Figure 10. Illustration of the metaphragma (**ph3**) in the propodeum (**T1**) of *Ampulex compressa*. **A.** Medial view, anterior to the right; **B.** Anteromedial view on **ph3-T2** – metaphragmo-second abdominal tergal muscle; **C.** Anteromedial view on **ph3**; **D.** Posterior view on the vertical part of propodeum. Scale bars: 0.6 mm (A), 0.3 mm (B, C), 0.9 mm (D).

The homology of the metanotal muscle, which we tentatively assign to **pl3lp-t3**, according to the HAO terminology, cannot be assured. In the HAO, it is described as fan-shaped and posterolaterally originating from the metapleuron. However, size, structure, and position of **pl3lp-t3** are different among the species examined (Figs 3D, 5C, D). In *Ampulex*, **pl3lp-t3** shows great similarity to the description of it by the HAO (wide, fan-shaped, and arises laterally from the metapleuron), whereas in Sphecidae, **pl3lp-t3** is very small and compact but still fan-shaped and located sublaterally. It appears to originate from the metanotum and to insert on the metapleu-

ron. Additional examination of **pl3lp-t3** in other specimens is required to resolve the homology of this muscle.

The muscle **s3-cx3** is clearly identifiable in *Sphex* (Fig. 4B). It is located ventrally to **fu3m-cx3** and might serve to strengthen the metacoxal function from the lower centre of the body. From **fu3m-cx3**, **s3-cx3** might be subdivided. This possibly forms a genus-specific character of *Sphex*, but not of the family Sphecidae.

First and second abdominal segment. The metaphragma is conspicuously absent in Sphecidae among all studied taxa. Nevertheless, **ph2m-ph3** (Fig. 3A) and **ph3-T2** (Fig. 3A–D) in Sphecidae are homologue muscles. The metaphragma is usually located between the metanotum and the first abdominal segment (Snodgrass 1942). The HAO describes the metaphragma as the site of origin of the mesophragmo-metaphragmal and metaphragmo-second abdominal tergal muscles. Although the third phragma was found to be absent in honeybees by Snodgrass (1942). However, Vilhelmsen et al. (2010) stated that most Hymenoptera have at least a weak laterally developed metaphragma. This has been observed in Mymarommatoidea (Terebrantia) and Chrysidoidea (Aculeata). Vilhelmsen et al. (2010) described a metaphragma medially continuous adjacent to the lateral metapleural apodeme for other apocritan taxa (i.e., Vespoidea, Trigonaloidea, Megalyroidea, Stephanoidea, Evanioidea, most Ichneumonoidea, and Apoidea: *Stangeella* (Sphecidae), *Pison* (Crabronidae), and *Ampulex* (Ampulicidae)). *Stangeella* and *Ampulex* were analysed by dissection but not figured. We cannot confirm this specific pattern for *Ampulex* (Fig. 10A–D). The absence of the metaphragma we observed in *Sceliphron* and *Sphex* may be a potential autapomorphy or an independent reduction. Consequently, further investigation of this phragma is highly recommended.

Conclusions

We recommend additional investigations of the structures and features presented in this paper. It would be of great value to analyse the tagmata and other characteristics in the family Heterogynaidae and additional species of Crabronidae, Ampulicidae, and Sphecidae. Due to the unresolved phylogenetic position of Heterogynaidae and the paraphyly of Crabronidae, the study of more species from these taxa might be desirable. Structural investigations of more species of Vespoidea and Chrysidoidea would be helpful for clarifying controversial assumptions about phylogenetic relationships within Aculeata. Structures of phylogenetic significance were mainly found in the metathorax, i.e., the metapleural apodeme, paracoxal ridge, metaphragma, and the origin and insertion of associated muscles. Future studies should also focus on: the muscles that insert into the legs, the posterior thoracic spiracle as well as the occlusor muscle in closely related species, and the four muscles described here for the first time in Sphecidae and Ampulicidae.

References

Aguiar AP, Deans AR, Engel MS, Forshage M, Huber JT, Jennings JT, Johnson NF, Lelej AS, Longino JT, Lohrmann V, Mikó I, Ohl M, Rasmussen C, Taeger A, Sick Ki Yu D (2013) Order Hymenoptera. In: Zhang Z-Q (Ed.) Animal biodiversity: an outline of higher-level classification and survey of taxonomic richness (addenda 2013). Zootaxa 3703: 51–62. https://doi.org/10.11646/zootaxa.3703.1.12

Alexander BA (1992) A cladistic analysis of the subfamily Philanthinae (Hymenoptera: Sphecidae). Systematic Entomology 17(2): 91–108. https://doi.org/10.1111/j.1365-3113.1992.tb00324.x.

Bohart RM, Menke AS (1976) Sphecid wasps of the world. A generic revision. University of California Press, Berkeley, Los Angeles, London, 695 pp. https://archive.org/details/bub_gb_FExMjuRhjpIC/page/n27

Branstetter MG, Danforth BN, Pitts JP, Faircloth BC, Ward PS, Buffington ML, Gates MW, Kula RR, Brady SG (2017) Phylogenomic Insights into the evolution of stinging wasps and the origins of ants and bees. Current Biology 27(7): 1019–1025. https://doi.org/10.1016/j.cub.2017.03.027

Brothers DJ, Carpenter JM (1993) Phylogeny of Aculeata: Chrysidoidea and Vespoidea (Hymenoptera). Journal of Hymenoptera Research 2(1): 227–304.

Debevec AH, Cardinal S, Danforth BN (2012) Identifying the sister group to the bees: a molecular phylogeny of Aculeata with an emphasis on the superfamily Apoidea. Zoologica Scripta 41(5): 527–535. https://doi.org/10.1111/j.1463-6409.2012.00549.x

Duncan CD (1939) A contribution to the biology of North American vespine wasps. Stanford University Publication, University Series Biology and Science 8: 1–272.

Faulwetter S, Vasileiadou A, Kouratoras M, Dailianis T, Arvanitidis C (2013) Micro-computed tomography: Introducing new dimensions to taxonomy. ZooKeys 263: 1–45. https://doi.org/10.3897/zookeys.263.4261

Fouad K, Libersat F, Rathmayer W (1994) The venom of the cockroach-hunting wasp *Ampulex compressa* changes motor thresholds: a novel tool for studying the neural control of arousal. Zoology 98: 23–34.

Friedrich F, Beutel RG (2008) The thorax of *Zorotypus* (Hexapoda, Zoraptera) and a new nomenclature for the musculature of Neoptera. Arthropod Structure & Development 37: 29–54. https://doi.org/10.1016/j.asd.2007.04.003

Friedrich F, Beutel RG (2010) Goodbye Halteria? The thoracic morphology of Endopterygota (Insecta) and its phylogenetic implications. Cladistics 26(6): 579–612. https://doi.org/10.1111/j.1096-0031.2010.00305.x

Garcia FH, Fischer G, Liu C, Audisio TL, Economo EP (2017) Next-generation morphological character discovery and evaluation: an X-ray micro-CT enhanced revision of the ant genus *Zasphinctus* Wheeler (Hymenoptera, Formicidae, Dorylinae) in the Afrotropics. ZooKeys 693: 33–93. https://doi.org/10.3897/zookeys.693.13012

Gignac PM, Kley NJ, Clarke JA, Colbert MW, Morhardt AC, Cerio D, Cost IN, Cox PG, Daza JD, Early CM, Echols MS, Henkelman RM, Herdina AN, Holliday CM, Li Z, Mahlow K, Merchant S, Müller J, Orsbon CP, Paluh DJ, Thies ML, Tsai HP, Witmer LM (2016) Diffusible iodine-based contrast-enhanced computed tomography (diceCT): an emerging tool for rapid, high-resolution, 3-D imaging of metazoan soft tissues. Journal of Anatomy 228: 889–909. https://doi.org/10.1111/joa.12449

Haspel G, Libersat F (2003) Wasp venom blocks central cholinergic synapses to induce transient paralysis in cockroach prey. Developmental Neurobiology 54(4): 628–637. https://doi.org/10.1002/neu.10195

Heraty JM (1989) Morphology of the mesosoma of *Kapala* (Hymenoptera: Eucharitidae) with emphasis on its phylogenetic implications. Canadian Journal of Zoology 67(1): 115–125. https://doi.org/10.1139/z89-018

Johnson BR, Borowiec ML, Chiu JC, Lee EK, Atallah J, Ward PS (2013) Phylogenomics resolves evolutionary relationships among ants, bees, and wasps. Current Biology 23: 2058–2062. https://doi.org/10.1016/j.cub.2013.08.050

Kawada R, Lanes GO, Azevedo CO (2015) Evolution of Metapostnotum in Flat Wasps (Hymenoptera, Bethylidae): Implications for Homology Assessments in Chrysidoidea. PLoS ONE10 (10): e0140051. https://doi.org/10.1371/journal.pone.0140051

Königsmann E (1978) Das phylogenetische System der Hymenoptera. Teil 4: Aculeata (Unterordnung Apocrita). Deutsche Entomologische Zeitschrift, Neue Folge 25: 365–435. https://doi.org/10.1002/mmnd.19780250408

Libersat F (2003) Wasp uses venom cocktail to manipulate the behavior of its cockroach prey. Journal of Comparative Physiology A 189(7): 497–508. https://doi.org/10.1007/s00359-003-0432-0

Liu S-P, Richter A, Stoessel A, Beutel RG (2019) The mesosomal anatomy of *Myrmecia nigrocincta* workers and evolutionary transformations in Formicidae (Hymenoptera). Arthropod Systematics & Phylogeny 77(1): 1–19. https://doi.org/10.26049/ASP77-1-2019-01

Lohrmann V, Ohl M, Bleidorn C, Podsialowski L (2008) Phylogenie der „Sphecidae" (Hymenoptera: Apoidea) basierend auf molekularen Daten. Mitteilungen der Deutschen Gesellschaft für allgemeine und angewandte Entomologie 16: 99–102.

Lomholdt O (1982) On the origin of the bees (Hymenoptera: Apidae, Sphecidae). Insect Systematics & Evolution 13(2): 185–190. https://doi.org/10.1163/187631282X00093

Maki T (1938) Studies on the thoracic musculature in insects. Memoirs of the Faculty of Science and Agriculture, Taihoku Imperial University 24(1): 1–343.

Matsuda R (1970) Morphology and Evolution of the Insect Thorax. Memoirs of the Entomological Society of Canada 102(S76): 5–431. https://doi.org/10.4039/entm10276fv

Metscher BD (2009) MicroCT for comparative morphology: simple staining methods allow high-contrast 3D imaging of diverse non-mineralized animal tissues. BMC Physiology 9: 11. https://doi.org/10.1186/1472-6793-9-11

Mikó I, Vilhelmsen L, Johnson NF, Masner L, Pénzes Z (2007) Skeletomusculature of Scelionidae (Hymenoptera: Platygastroidea): head and mesosoma. Zootaxa 1571: 1–78. https://doi.org/10.11646/zootaxa.1571.1.1

O'Neill KM (2001) Solitary wasps: natural history and behavior. Cornell University Press, Ithaca, NY, 406 pp.

Ohl M, Bleidorn C (2006) The phylogenetic position of the enigmatic wasp family Heterogynaidae based on molecular data, with description of a new, nocturnal species (Hymenoptera: Apoidea). Systematic Entomology 31(2): 321–337. https://doi.org/10.1111/j.1365-3113.2005.00313.x

Ohl M, Engel MS (2007) Die Fossilgeschichte der Bienen und ihrer nächsten Verwandten (Hymenoptera: Apoidea). Denisia 20: 687–700.

Ohl M, Spahn P (2010) A cladistic analysis of the cockroach wasps based on morphological data (Hymenoptera: Ampulicidae). Cladistics 26: 49–61. https://doi.org/10.1111/j.1096-0031.2009.00275.x

Peters RS, Meyer B, Krogmann L, Borner J, Meusemann K, Schütte K, Niehuis O, Misof B (2011) The taming of an impossible child: a standardized all-in approach to the phylogeny of Hymenoptera using public database sequences. BMC Biology 9: 55. https://doi.org/10.1186/1741-7007-9-55

Peters RS, Krogmann L, Mayer C, Donath A, Gunkel S, Meusemann K, Kozlov A, Podsiadlowski L, Petersen M, Lanfear R, Diez PA, Heraty J, Kjer KM, Klopfstein S, Meier R, Polidori C, Schmitt T, Liu S, Zhou X, Wappler T, Rust J, Misof B, Niehuis O (2017) Evolutionary history of the Hymenoptera. Current Biology 27(7): 1013–1018. https://doi.org/10.1016/j.cub.2017.01.027

Porto DS, Almeida EAB, Vilhelmsen L (2016) Comparative morphology of internal structures of the mesosoma of bees with an emphasis on the corbiculate clade (Apidae: Apini). Zoological Journal of the Linnean Society 179: 303–337. https://doi.org/10.1111/zoj.12466

Prentice MA (1998) The comparative morphology and phylogeny of the apoid wasps (Hymenoptera: Apoidea). Ph.D. Dissertation, University of California, Berkeley, 1439 pp.

Pulawski WJ (2020) Catalog of Sphecidae (see "Number of Species" via https://www.calacademy.org/scientists/projects/catalog-of-sphecidae)

Rasnitsyn AP (1988) An Outline of Evolution of the Hymenopterous Insects (Order Vespida). Oriental Insects 22: 115–145. https://doi.org/10.1080/00305316.1988.11835485

Ronquist F, Rasnitsyn AP, Roy A, Eriksson K, Lindgren M (1999) Phylogeny of the Hymenoptera: A cladistic reanalysis of Rasnitsyn's (1988) data. Zoologica Scripta 28: 13–50. https://doi.org/10.1046/j.1463-6409.1999.00023.x

Sann M, Niehuis O, Peters RS, Mayer C, Kozlov A, Podsiadlowski L, Bank S, Meusemann K, Misof B, Bleidorn C, Ohl M (2018) Phylogenomic analysis of Apoidea sheds new light on the sister group of bees. BMC evolutionary biology 18(1): 71. https://doi.org/10.1186/s12862-018-1155-8

Schmidt JO (2016) The sting of the wild. Johns Hopkins University Press, Baltimore, 280 pp.

Seltmann KC, Yoder MJ, Mikó I, Forshage M, Bertone MA, Agosti D, Austin AD, Balhoff JP, Borowiec ML, Brady SG, Broad GR, Brothers DJ, Burks RA, Buffington ML, Campbell HM, Dew KJ, Ernst AF, Fernández-Triana JL, Gates MW, Gibson GAP, Jennings JT, Johnson NF, Karlsson D, Kawada R, Krogmann L, Kula RR, Mullins

PL, Ohl M, Rasmussen C, Ronquist F, Schulmeister S, Sharkey MJ, Talamas E, Tucker E, Vilhelmsen L, Ward PS, Wharton RA, Deans AR (2012) A hymenopterists' guide to the Hymenoptera anatomy ontology: utility, clarification, and future directions. Journal of Hymenoptera Research 27: 67–88. https://doi.org/10.3897/jhr.27.2961

Sharkey MJ, Carpenter JM, Vilhelmsen L, Heraty J, Liljeblad J, Dowling APG, Schulmeister S, Murray D, Deans AR, Ronquist F, Krogmann L, Wheeler WC (2012) Phylogenetic relationships among superfamilies of Hymenoptera. Cladistics 28(1): 80–112. https://doi.org/10.1111/j.1096-0031.2011.00366.x

Snodgrass RE (1942) The skeleto-muscular mechanisms of the honey bee. Smithsonian Miscellaneous Collections 103(2): 1–120. http://hdl.handle.net/10088/22771

Vilhelmsen L, Mikó I, Krogmann L (2010) Beyond the wasp-waist: structural diversity and phylogenetic significance of the mesosoma in apocritan wasps (Insecta: Hymenoptera). Zoological Journal of the Linnean Society 159(1): 22–294. https://doi.org/10.1111/j.1096-3642.2009.00576.x

Williams FX (1942) *Ampulex compressa* (Fabr.), A cockroach-hunting wasp introduced from New Caledonia into Hawaii. Proceedings of the Hawaiian Entomological Society 11(2): 221–233. http://hdl.handle.net/10125/16067

Willsch M (2019) Micro-computed tomography scanning of the mesosomal musculature in Apoidea (aculeate Hymenoptera) – segmented structures and raw data. [Dataset]. Data Publisher: Museum für Naturkunde Berlin (MfN) – Leibniz Institute for Research on Evolution and Biodiversity. https://doi.org/10.7479/dft0-yy6m

Yoder MJ, Mikó I, Seltmann KC, Bertone MA, Deans AR (2010) A Gross Anatomy Ontology for Hymenoptera, PLOS ONE 5(12): e15991. https://doi.org/10.1371/journal.pone.0015991

Zimmermann D, Vilhelmsen L (2016) The sister group of Aculeata (Hymenoptera) – evidence from internal head anatomy, with emphasis on the tentorium. Arthropod Systematics & Phylogeny 74(2): 195–218. https://curis.ku.dk/portal/files/171586094/05_asp_74_2_zimmermann_195_218.pdf

Supplementary material 1

Table S1

Authors: Maraike Willsch, Frank Friedrich, Daniel Baum, Ivo Jurisch, Michael Ohl

Data type: Excel file

Explanation note: Provision of Universal Resource Identifiers (URIs) referring to structures mentioned in the paper. Automatic creation by using the Hymenoptera Anatomy Ontology "analyzer" (http://api.hymao.org/projects/32/public/ontology/analyze).

Link: https://doi.org/10.3897/dez.67.49493.suppl1